

Article

Biocatalysis at Extreme Temperatures: Enantioselective Synthesis of both Enantiomers of Mandelic Acid by Transesterification Catalyzed by a Thermophilic Lipase in Ionic Liquids at 120 °C

Jesús Ramos-Martín, Oussama Khiari, Andrés R. Alcántara *  and Jose María Sánchez-Montero *

Department of Chemistry in Pharmaceutical Sciences, Pharmacy Faculty, Complutense University of Madrid (UCM), Ciudad Universitaria, Plaza de Ramon y Cajal, s/n., 28040 Madrid, Spain; rivasfarma@hotmail.com (J.R.-M.); oussama.khiari@gmail.com (O.K.)

* Correspondence: andalcan@ucm.es (A.R.A.); jmsm@ucm.es (J.M.S.-M.);

Tel.: +34-91-394-1820 (A.R.A.); +34-91-394-1839 (J.M.S.-M.)

Received: 15 August 2020; Accepted: 11 September 2020; Published: 14 September 2020



Abstract: The use of biocatalysts in organic chemistry for catalyzing chemo-, regio- and stereoselective transformations has become an usual tool in the last years, both at lab and industrial scale. This is not only because of their exquisite precision, but also due to the inherent increase in the process sustainability. Nevertheless, most of the interesting industrial reactions involve water-insoluble substrates, so the use of (generally not green) organic solvents is generally required. Although lipases are capable of maintaining their catalytic precision working in those solvents, reactions are usually very slow and consequently not very appropriate for industrial purposes. Increasing reaction temperature would accelerate the reaction rate, but this should require the use of lipases from thermophiles, which tend to be more enantioselective at lower temperatures, as they are more rigid than those from mesophiles. Therefore, the ideal scenario would require a thermophilic lipase capable of retaining high enantioselectivity at high temperatures. In this paper, we describe the use of lipase from *Geobacillus thermocatenolatus* as catalyst in the ethanolysis of racemic 2-(butyryloxy)-2-phenylacetic to furnish both enantiomers of mandelic acid, an useful intermediate in the synthesis of many drugs and active products. The catalytic performance at high temperature in a conventional organic solvent (*isooctane*) and four imidazolium-based ionic liquids was assessed. The best results were obtained using 1-ethyl-3-methyl imidazolium tetrafluoroborate (EMIMBF₄) and 1-ethyl-3-methyl imidazolium hexafluorophosphate (EMIMPF₆) at temperatures as high as 120 °C, observing in both cases very fast and enantioselective kinetic resolutions, respectively leading exclusively to the (*S*) or to the (*R*)-enantiomer of mandelic acid, depending on the anion component of the ionic liquid.

Keywords: *Geobacillus thermocatenolatus*; lipases; ethanolysis; ionic liquids; kinetic resolution; mandelic acid

1. Introduction

Employing biocatalysts in organic chemistry, either alone [1,2] or combined with chemical catalysts [3,4] for developing selective transformations has become a common tool in the last years [5,6]. This is based on the extremely enzymatic precision (chemo-, regio- and stereoselectivity) acquired when applied in biotransformations not only at lab, but also at industrial scale [7–11], being used mainly in pharma industry [12–17]. Moreover, moving from chemical catalysis to biocatalysis leads to an increase in process sustainability—given that biocatalysis and green chemistry usually go hand-in-hand [2,17–19].

One of the green credentials of biocatalysis derives from the fact that biotransformations can be conducted under very mild reaction conditions, e.g., atmospheric pressure, room temperature or aqueous media. However, harsh conditions required for many industrial processes—such as high temperature and/or the use of organic (co)solvents—may impede the use of some enzymes. To address these drawbacks, using thermotolerant biocatalysts obtained from thermophilic organisms is an excellent alternative [20–23], as these thermozyms can efficiently work at very high temperatures [24,25] and are generally very resistant to organic solvent-promoted denaturation [26,27]. Among all the arsenal of enzymes available for being used in biotransformations, lipases (triacylglycerol hydrolases, EC 3.1.1.3) are one of the most frequently applied, as they are easily available, do not need cofactors and display a wide range of substrate recognition [28–31]. Furthermore, their ability for working in almost anhydrous organic solvents allows conducting reactions in the sense of synthesis instead of hydrolysis, therefore favoring the transformation of many organic compounds, which are generally water-insoluble and thus reverting the original enzymatic selectivity [32–34].

The use of lipases from thermophiles has been frequently reported [23,35,36]. Among them, the term “thermoalkaline (TA) lipases” describes some enzymes resistant not only to temperature (70–80 °C) but also to the presence of alkaline media (pH values between 8 and 10) [36]. These enzymes possess a peculiar feature in their 3D structure due to the presence of a relatively large lid domain (around 70 residues) formed by two alpha-helices (α_6 and α_7) [37], so that the opening of this lid domain upon exposing the active site requires a significant conformational change [38]. One of the most representative examples of TA lipases is that one from *Geobacillus* (formerly *Bacillus* [39]) *thermocatenulatus*. From this microorganism, Schmidt-Dannert et al. [40–42] described two lipases, namely BTL1 and BTL2. The latter was crystallized in its open form by Carrasco-Lopez et al. [37,43]. The stereoselectivity of BTL2 towards 29 chiral substrates was initially tested by Liu et al. [44], reporting only good results for the acylation of 1-phenylethanol and 1-phenylpropanol with vinyl acetate (as well as for the hydrolysis of the corresponding esters). Later, this enzyme—immobilized on different supports via diverse methodologies—has been extensively tested on different substrates, some of them chiral [45–64], generally with moderate results. Additionally, chemical [55,58,65–67] and genetic [56,68–71] modifications of BTL2 lipase for improving its catalytic behavior (typically, to reduce the steric hindrance around the active site) have been also reported. Finally, different papers in recent literature have employed the reported 3D structure of BTL2 for performing molecular simulations aiming to rationalize its catalytic performance and stability [38,72–74].

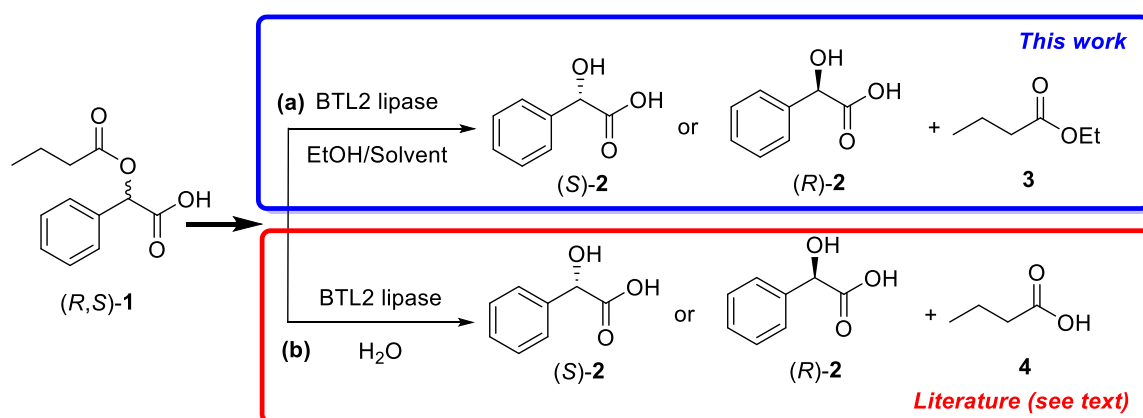
Although TA lipases are very resistant to organic solvents and high temperatures, the boiling point of the solvents clearly limits the maximum operational temperature. In this sense, the use of RTILs (room-temperature ionic liquids) can be very convenient, as they display very high boiling points and have been proven to be compatible with enzymatic catalysis [75–78]. RTILs (organic salts consisting of an organic cation and a polyatomic inorganic anion, liquid under 100 °C), are broadly regarded as green solvents [79], as they have extremely high enthalpies of vaporization (making them effectively nonvolatile), as well as high chemical and thermal stabilities and remarkable solvating power, so that they can be safely used at high temperature. However, the large number of steps required for their synthesis, sometimes demanding the use of non-renewable crude oil sources and some toxic intermediates, may alter their consideration as eco-friendly solvents [80]. On the other hand, the high cost of RTILs can be compensated by their easy recovery from the reaction media (by simply extracting with (green) organic solvents), which allows to reuse them several times [78].

Remarkably, as their rigidity is higher, thermophilic enzymes are more stereoselective when used at the optimum reaction temperature of the corresponding mesophilic counterparts, which usually is far below their own ideal value [23]. As temperature increases, reaction rate also increases as the thermozyms are approaching its optimal value, but at the expense of a stereoselectivity fall (because of the higher enzymatic flexibility) down to the total loss of activity and enantioselectivity once a certain maximum temperature is overpassed. Finding a thermophilic enzyme retaining its activity and stereodiscrimination capability at very high temperature would be highly desirable.

To illustrate this point, we present the results obtained in the kinetic resolution of 2-(butyryloxy)-2-phenylacetic acid via ethanolysis catalyzed by BTL2 using different ionic liquids (1-butyl-3-methyl imidazolium tetrafluoroborate (BMIMBF₄), 1-butyl-3-methyl imidazolium hexafluorophosphate (BMIMPF₆), 1-ethyl-3-methyl imidazolium tetrafluoroborate (EMIMBF₄) and 1-ethyl-3-methyl imidazolium hexafluorophosphate (EMIMPF₆) at high temperatures (90 and 120 °C), comparing the results with those obtained with a conventional organic solvent (*isooctane*).

2. Results

The kinetic resolution of racemic 2-(butyryloxy)-2-phenylacetic acid (*R,S*)-1 via ethanolysis to yield pure enantiomers of mandelic acid (*R*) or (*S*)-2 was selected as test reaction to check the performance of BTL2, as depicted in Scheme 1a.



Scheme 1. Kinetic resolution of 2-(butyryloxy)-2-phenylacetic acid (*R,S*)-1 via ((a), this work) BTL2-catalyzed ethanolysis or ((b), literature) BTL2-catalyzed hydrolysis.

(*R*)-mandelic acid and analogs are key synthons in the preparation of several drugs or biologically active compounds, being in the core of semi-synthetic antibiotics (cephalosporins as cefamandole [81] or penicillins as MA-6-APA II [82]) or anticholinergic drugs (such as oxybutynin [83] and homatropine [84]). Moreover, derivatives of (*R*)-mandelic acid have been also used as chiral synthons in the preparation of some drugs with different therapeutic activities: platelet/antithrombotic agents (clopidogrel [85]), vasodilator (cyclandelate [86]), antitumor (complex of *cis*-[Pt(2-(α -hydroxy)benzylbenzimidazole)]₂Cl₂] [87], antiobesity [88,89] or CNS-stimulant dopaminergic agents ((*R*)-pemoline [90]). Conversely, (*S*)-mandelic acid is used for the production of non-steroidal anti-inflammatory drugs such as deracoxib and celecoxib [91].

In this paper, we present the first reported example of kinetic resolution of (*R,S*)-1, leading to enantiopure mandelic acid, by ethanolysis catalyzed by BTL2 (Scheme 1a) at very high reaction temperature. Selection of (*R,S*)-1 as model substrate was based in many previous studies in which BTL2 (mainly immobilized) had been used for catalyzing its stereoselective hydrolysis (Figure 1b) [45,48,49,51,56,58]. In these papers, only low to moderate enantioselectivity is generally observed in the hydrolysis of (*R,S*)-1, and, remarkably, the enzymatic stereobias, leading to either (*R*)-2 or (*S*)-2, depends on the type of support and the methodology used for the immobilization.

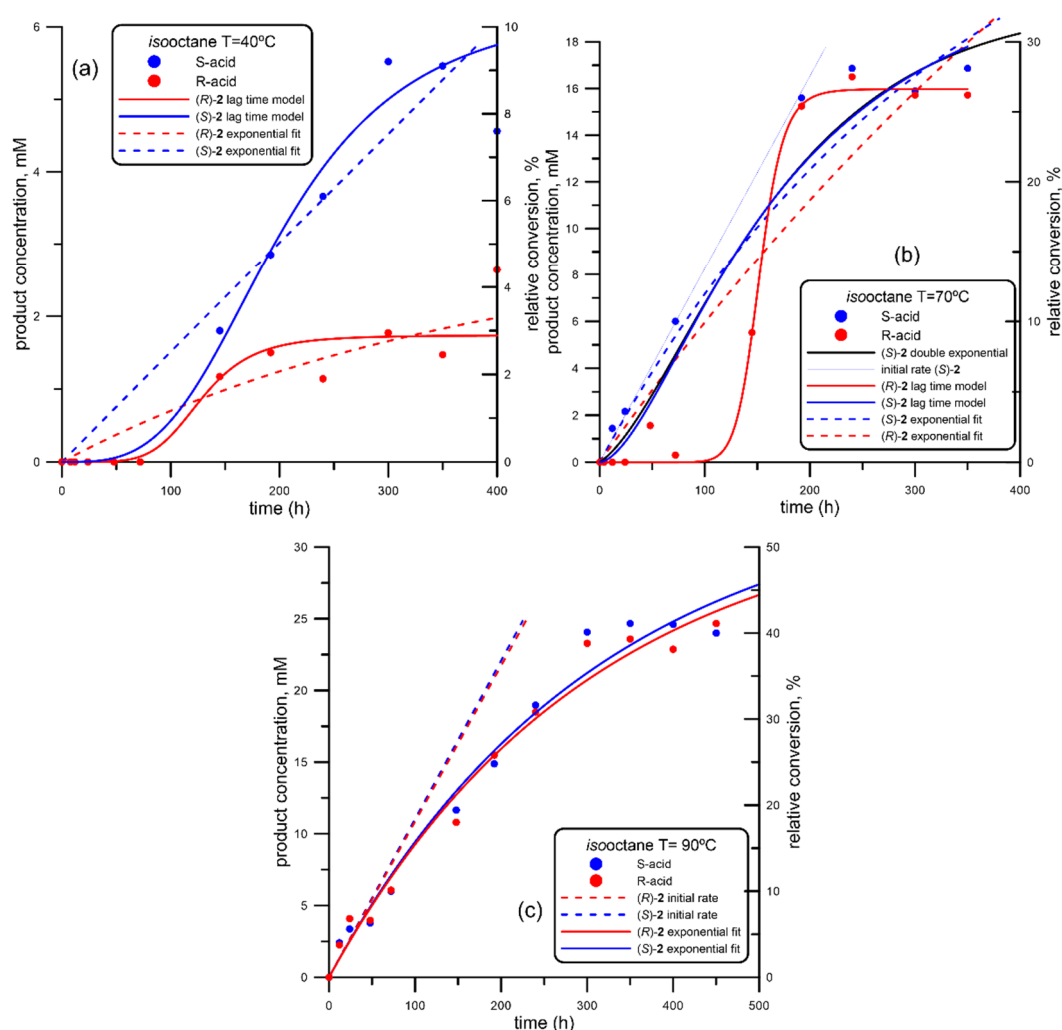


Figure 1. Progress curve of the lipase-form *Geobacillus thermocatenulatus* (BTL2)-catalyzed production of both enantiomers of mandelic acid ((*R*)-acid, in red; (*S*)-acid, in blue) via ethanolysis of racemic 2-(butyryloxy)-2-phenylacetic acid (*R,S*)-**1**, using isooctane as organic solvent at different temperatures. (a) 40 °C; (b) 70 °C; (c) 90 °C.

2.1. Ethanolysis of (*R,S*)-**1** in Isooctane at Different Temperatures

Nevertheless, hydrolysis is not a good alternative for checking the real thermostolerance of a lipase, as the stability of these enzymes is much higher when they are working on organic solvents [26,33,75]. Thus, we decided to use a water-free reaction media, selecting EtOH as nucleophile instead of water and a water-insoluble organic solvent (Figure 1a). Opting for EtOH was based on our previous studies on esterification of phthalic acids with BTL2 [92], and it has been very recently substantiated by Shehata et al. [38]; indeed, these authors have published a molecular dynamics (MD) simulation of the effect of different polar and nonpolar solvents on the thermostability and lid-opening of BTL2, reporting that the open (active) conformation of BLT2 is more stable in EtOH than in MeOH and even water. Additionally, this same study revealed that the overall lipase structure became more stable in nonpolar organic solvents, while it was destabilized in polar solvents except EtOH. Thus, it seems reasonable to use EtOH as nucleophile. On the other hand, isooctane (2,2,4-trimethylpentane) was the classical organic solvent selected for comparative reasons, as we had previously described its effectiveness in lipase-promoted catalysis [93–98]. This solvent is considered usable according to the Pfizer solvent selection guide for medicinal chemistry [99].

Thus, following the experimental procedure described in Section 4.2, the ethanolysis of (*R,S*)-1 was tested at three different temperatures (40, 70 and 90 °C). The progress curves are depicted in Figure 1.

As can be seen from Figure 1a, the reaction at 40 °C proceeds very slowly, reaching a global conversion of around 10% for (*S*)-2 after 400 h and 3–4% for the (*R*)-2 counterpart. In addition, a very strong lag-time is observed for both enantiomers, not detecting any trace of ethanolysis of (*R,S*)-1 in the first 75 h. A similar pattern was observed in the generation of (*R*)-2 at 70 °C (Figure 1b); in any case, no lag-time was observed for (*S*)-2 at that temperature and also for both enantiomers at 90 °C (Figure 1c), following a typical exponential grow. Thus, all the progress curves were adjusted using the program INRATE implemented inside SIMFIT fitting package (version 7.6, Release 9), a free-of-charge Open Source software for simulation, curve fitting, statistics and plotting [100] (accessible at <https://simfit.org.uk/simfit.html>). Using this program, data were fitted either to lag-time kinetics or to standard single exponential growing model. From these mathematical fittings, several parameters were calculated (shown in Table 1) and used to quantify the activity and enantioselectivity of BTL2 in the kinetic resolution of (*R,S*)-1 via ethanolysis.

Table 1. Quantitative assessment of the ethanolysis of racemic 2-(butyryloxy)-2-phenylacetic acid (*R,S*)-1 catalyzed by BTL2 using *isooctane* as organic solvent at different temperatures.

Medium	T (°C)	V _S ¹	V _R ¹	VS/V _R	t _{MAX} ⁴	[C] max ⁵	P ⁶	[(<i>S</i>)-2] ⁷	[(<i>R</i>)-2] ⁷	E ⁷	
#1	<i>isooctane</i>	40	0.015 ² 0.027 ³	0.008 ² 0.014 ³	1.9 ² 1.9 ³			0	0	nd	
#2	<i>isooctane</i>	70	0.083 ²	0.063 ² 0.332 ³	1.32 ²	24	2.26	0.09	1.44	0	>200
#3	<i>isooctane</i>	90	0.110 ²	0.108 ²	1.02 ²			4.0	3.75	nd	

¹ initial rate (mM/h). ² single exponential model. ³ lag-time model. ⁴ higher reaction time (h) at which only one enantiomer is detected. ⁵ concentration (mM) of the only isomer detected at that higher reaction time. ⁶ productivity (mM acid/h) at the higher reaction time. ⁷ enantiomeric ratio, calculated at 12 h.

As commented before, reaction was extremely slow at 40 °C; increasing the temperature up to 70 °C (Figure 1b), the reaction rate increased very markedly, and the catalytic performance for both enantiomers was clearly different: while the generation (*S*)-2 was detected from the early reaction stages and follows a single exponential model, it is not until 100 h when (*R*)-2 was clearly detected, quickly growing after this point to reach similar conversion values than those observed for (*S*)-2 after 200 h. When the temperature was increased up to 90 °C (Figure 1c), both enantiomers were produced by a similar pattern, at the same initial rate (Table 1, entry #3) and reaching similar conversion degrees (around 40%) after 500 h, with no enantioselectivity at all. Higher temperatures were not tested as it would mean approaching the boiling point of *isooctane* (99.6 °C)

Overall, best results are those obtained at 70 °C at short reaction times. In fact, inside the time interval from 0 to 75 h, the enantioselectivity is almost perfect, although at the expenses of a low overall conversions (around 10%, Figure 1b). Nevertheless, as results with this organic solvent were quite unsatisfactory, room-temperature ionic liquids (RTILs) were subsequently tested.

2.2. Ethanolysis of (*R,S*)-1 in RTILs at Different Temperatures

As commented in the Introduction, RTILs are fully compatible with enzymatic catalysis [75–78]. The most popular RTILs are those based on imidazolium cations [101,102], being 1-butyl-3-methyl imidazolium tetrafluoroborate (BMIMBF₄), 1-butyl-3-methyl imidazolium hexafluorophosphate (BMIMPF₆), 1-ethyl-3-methyl imidazolium tetrafluoroborate (EMIMBF₄) and 1-ethyl-3-methyl imidazolium hexafluorophosphate (EMIMPF₆) probably the first ones to be broadly commercialized. Their properties have been profusely described, especially including their complete miscibility with EtOH [103–110], the other main component of the reaction medium, used both as cosolvent and nucleophile. As these RTILs possess a very high boiling point, the use of their mixtures with EtOH allows using these binary mixtures at high reaction temperatures, without any noticeable EtOH

evaporation. Hence, ethanolsis of (*R*, *S*)-1 was tested at two different temperatures, 90 °C (similar to the maximum tested with *isooctane*) and 120 °C, a temperature higher than the boiling point of the organic solvent. The results are depicted in Figures 2–5. Table 2 summarizes the parameters obtained from the fitting of the corresponding progress curves.

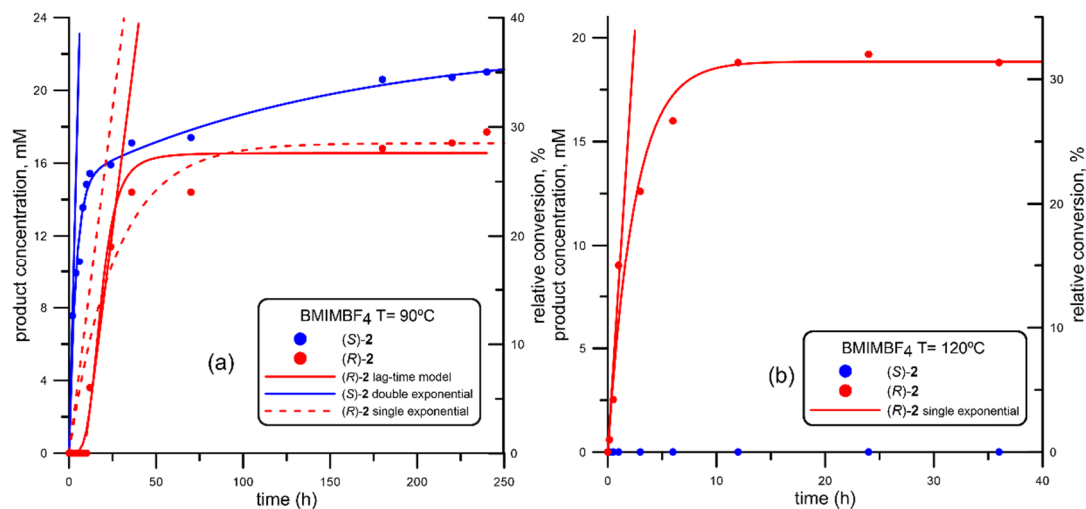


Figure 2. Progress curve of the BTL2-catalyzed production of both enantiomers of mandelic acid ((*R*)-acid, in red; (*S*)-acid, in blue) via ethanolsis of racemic 2-(butyryloxy)-2-phenylacetic acid (*R*, *S*)-1, using 1-butyl-3-methyl imidazolium tetrafluoroborate (BMIMBF₄) at different temperatures. (a) 90 °C; (b) 120 °C. Fitting parameters shown in Table 2, corresponding to entries #4 (BMIMBF₄ at 90 °C) and #5 (BMIMBF₄ at 120 °C).

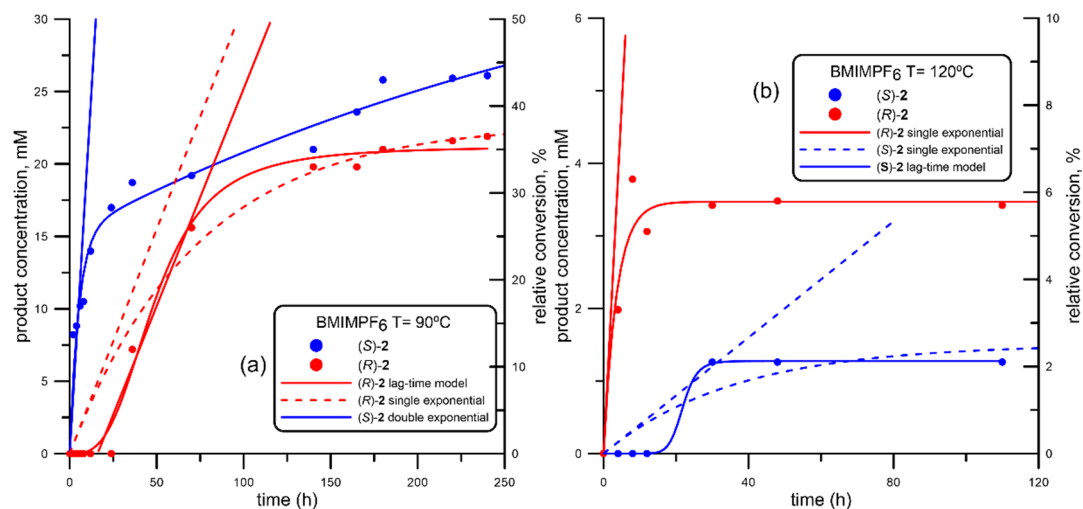


Figure 3. Progress curve of the BTL2-catalyzed production of both enantiomers of mandelic acid ((*R*)-acid, in red; (*S*)-acid, in blue) via ethanolsis of racemic 2-(butyryloxy)-2-phenylacetic acid (*R*, *S*)-1, using 1-butyl-3-methyl imidazolium hexafluorophosphate (BMIMPF₆) at different temperatures. (a) 90 °C; (b) 120 °C. Fitting parameters shown in Table 2, corresponding to entries #6 (BMIMPF₆ at 90 °C) and #7 (BMIMPF₆ at 120 °C).

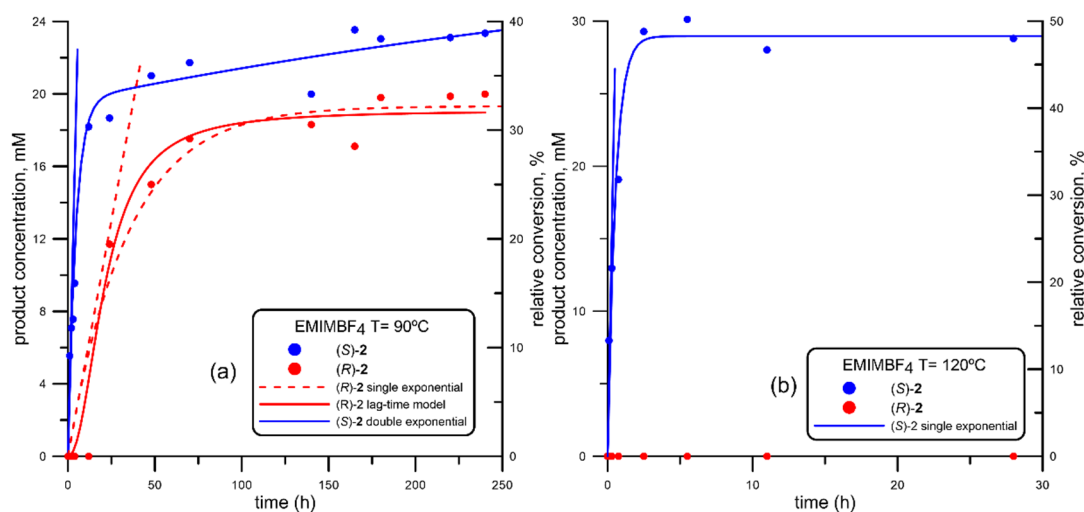


Figure 4. Progress curve of the BTL2-catalyzed production of both enantiomers of mandelic acid ((*R*)-acid, in red; (*S*)-acid, in blue) via ethanolsis of racemic 2-(butyryloxy)-2-phenylacetic acid (*R*, *S*)-**1**, using 1-ethyl-3-methyl imidazolium tetrafluoroborate (EMIMBF₄) at different temperatures. (a) 90 °C; (b) 120 °C. Fitting parameters shown in Table 2, corresponding to entries #8 (EMIMBF₄ at 90 °C) and #9 (EMIMBF₄ at 120 °C).

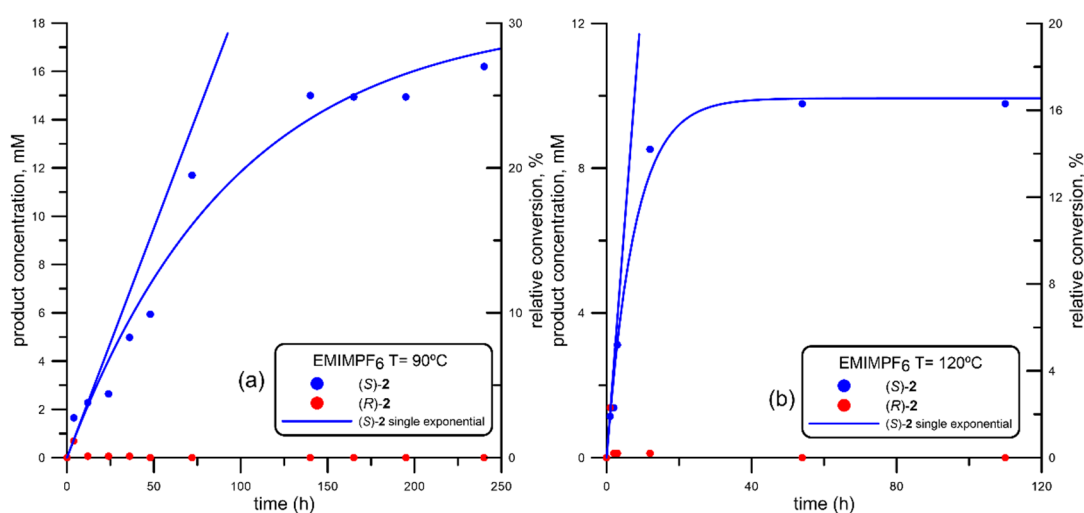


Figure 5. Progress curve of the BTL2-catalyzed production of both enantiomers of mandelic acid ((*R*)-acid, in red; (*S*)-acid, in blue) via ethanolsis of racemic 2-(butyryloxy)-2-phenylacetic acid (*R*, *S*)-**1**, using 1-ethyl-3-methyl imidazolium hexafluorophosphate (EMIMPF₆) at different temperatures. (a) 90 °C; (b) 120 °C. Fitting parameters shown in Table 2, corresponding to entries #9 (EMIMPF₆ at 90 °C) and #10 (EMIMPF₆ at 120 °C).

Table 2. Quantitative assessment of the ethanolysis of racemic 2-(butyryloxy)-2-phenylacetic acid (*R,S*)-1 catalyzed by BTL2 using different room-temperature ionic liquids (RTILs) at different temperatures.

	RTIL	T (°C)	V _S ¹	V _R ¹	V _{MAX} /V _{min} ²	t _{MAX} ³	[C] max ⁴	P ⁵	[(S)-2] ⁶	[(R)-2] ⁶	E ⁶
#4	BMIM BF ₄	90	3.85	0.76	5.1	10	13.6	1.36	15.42	13.6	1.1
#5	BMIM BF ₄	120	-	8.14	-	36	18.8	0.52	0	18.8	>200
#6	BMIM-PF ₆	90	2.0	0.31	6.4	24	17.0	0.71	14.0	0	>200
#7	BMIM-PF ₆	120	0.04	0.96	24	8	6.3	0.79	0	3.06	>200
#8	EMIM-BF ₄	90	4.08	0.52	7.8	12	18.2	3.03	18.2	0	>200
#9	EMIM-BF ₄	120	53.4	0	-	2.5	29.2	11.7	28.1	0	>200
#10	EMIM-PF ₆	90	1.86	-	-	240	16.2	0.81	2.28	0.06	51.3
#11	EMIM-PF ₆	120	1.3	-	-	54	9.8	0.18	8.52	0	>200

¹ initial rate (mM/h); ² V_S/V_R in all cases except for entries #5 and #7, when it should be V_R/V_S; ³ higher reaction time (h) at which only one enantiomer is detected; ⁴ concentration (mM) of the only isomer detected at that higher reaction time; ⁵ productivity (mM acid/h) at the higher reaction time; ⁶ enantiomeric ratio, calculated at 12 h.

2.2.1. Ethanolysis of (*R,S*)-1 Using RTILs Based on 1-Butyl-3-methyl Imidazolium (BMIM) as Solvent

When the tetrafluoroborate (BMIMBF₄) solvent was used (Figure 2), it can be observed how using the lower reaction temperature (90 °C, Figure 2a) led to a different kinetic behavior in the generation of both enantiomers of mandelic acid. In fact, as the (*S*)-acid (in blue) was detected from the earlier reaction stages, the correspondent (*R*)-acid (in red) was not produced until a lag-time of around 12 h had been overpassed, experimenting a rapid increase in its production leading to an overall sigmoid curve (Figure 2a, red solid line); remarkably, a similar initial rate (V_S = 3.85 mM/h, Table 2) was calculated considering a single exponential model (Figure 2a, red dotted line) or the sigmoid lag-time model, red solid line). In this case, (*S*)-acid (in blue) was the best-recognized enantiomer, as also observed using *isooctane* (Figure 1), although for BMIMBF₄ the initial rate was 35 times higher than that observed for *isooctane* (V_S = 0.11 mM/h, Table 1). Furthermore, the reaction in this RTIL was not only faster, but also more enantioselective than in *isooctane*, as the lag-time observed for the generation of the (*R*)-acid allowed the production of exclusively (*S*)-2 at the first stages of the reaction (t_{MAX} 10 h, [(*S*)-2]_{MAX} 13.6%, corresponding to 22.7% conversion).

Another interesting aspect to be taken into account is that, while the generation (*R*)-2 remained constant after a certain reaction time (around 30% after 50 h, according to the sigmoid fitting), the production of (*S*)-2 was slowly increasing after this time, although at a lower reaction rate than that observed at the early stages; that is the reason the overall (*S*)-2 production followed a double exponential fitting. This slower second reaction rate could be caused by an inhibition promoted by the increasing amounts of (*R*)-2 present in the reaction media, as the slope change in the (*S*)-2 production is observed only after a certain accumulation of (*R*)-2.

However, when performing the ethanolysis at 120 °C (Figure 2b), the observed reaction pattern was radically different from that obtained at 90 °C, as only the (*R*) enantiomer of mandelic acid was produced through a fast single exponential fit, displaying an initial rate (V_R = 8.14 mM/h, Table 2) twice that one obtained for the preferentially recognized (*S*)-2 at 90 °C. Indeed, the reaction did not progress after 40 h, and no traces of (*S*)-2 were detected under these conditions, so that the enantioselectivity was complete, leading to an overall conversion of around 30%.

An inversion in the stereobias of BTL2 in the recognition of both enantiomers of mandelic acid had been previously reported, although in the hydrolysis of (*R,S*)-1 and associated with the different methodology and support used for the immobilization of this lipase [45,47–49], as already mentioned in the Introduction. A simple explanation of this modification in the enantiodiscrimination of BTL2 upon increasing the temperature would demand a detailed computational study, which is out of the scope of this manuscript.

The results of the ethanolysis of (*R,S*)-1 using BMIMPF₆ are shown in Figure 3.

As can be seen, the behavior was similar to that observed using BMIMBF₄; at 90 °C (Figure 3a), the (*S*) enantiomer of mandelic acid is quickly detected, once again following a double exponential fit, at a smaller initial rate than that one obtained using BMIMBF₄, but also higher if compared to

that calculated using *isooctane* (Table 1). Similarly, the inversion in the stereobias at 120 °C is also detected, but now the reaction proceeded very poorly compared to that depicted in Figure 2b, as only a maximum of 6% conversion is detected for (*R*)-2.

2.2.2. Ethanolysis of (*R*, *S*)-1 Using RTILs Based on 1-Ethyl-3-methyl Imidazolium (EMIM) as Solvent

The results obtained using RTILs in which 1-ethyl-3-methyl imidazolium (EMIM) is the cation are shown in Figures 4 and 5. More concretely, Figure 4 shows the reaction progress curves using EMIMBF₄ at 90 °C (Figure 4a) and 120 °C (Figure 4b).

Comparing Figure 4a (EMIMBF₄) with Figure 2a (BMIMBF₄), a similar comportment is observed. As depicted in Figure 4a, the lag-time for the detection of (*R*)-2 was slightly higher than that observed using BMIMPF₄ and also the initial rate (4.08 vs 3.85 mM h⁻¹, Table 2), so that it was possible to detect only (*S*)-2 in the first 12 hours, reaching a concentration of 18.2 mM (around 30% conversion) with complete enantioselectivity. Once again, as the reaction proceeded and the (*R*)-2 enantiomer was being produced (lag-time and single exponential models almost similar), the rate of production of (*S*)-2 was reduced, so that once again the overall behavior for (*R*)-2 could be fitted to a double exponential curve.

When the reaction temperature is increased up to 120 °C (Figure 4b), a very fast kinetic resolution can be observed. In fact, the initial rate in the generation of (*S*)-2 ($V_S = 53.4$ mM h⁻¹, Table 2) was one order of magnitude higher than that obtained at 90 °C; moreover, no traces of (*R*)-2 were detected during the whole reaction time, so that the shape of the progress curve fits to a single exponential plot leading to almost 50% conversion (the maximum for a kinetic resolution) in only 2.5 hours.

Results obtained using EMIMPF₆ as solvents are depicted in Figure 5. As can be seen, at both temperatures only small traces of (*R*)-2 were detected, while the generation of (*S*)-2 followed single exponential kinetics. At 90 °C, the kinetic resolution observed using this solvent (Figure 5a) was slower (V_S around one half, See Table 2, entries #8 vs #10) than that obtained with EMIMBF₄ (Figure 4a), although this fact was compensated with an absence of production of (*R*)-2, leading to 30% conversion after 250 h. When increasing the temperature to 120 °C (Figure 5b), the kinetic resolution was slightly slower, and the maximum conversion was half that obtained at 90 °C.

3. Discussion

It is generally accepted that enzymes in RTILs are more active and stable as the hydrophobicity of the RTIL increases (see the review from Liu and co-workers [75], as well as the references cited therein). This fact is commonly related to the higher preservation of the essential water layer surrounding the enzyme structure, resulting in a decrease of the protein–ion interactions with a concomitant reduction of enzyme denaturation [76]. Therefore, the use of water-immiscible RTILs, more hydrophobic than the corresponding water-soluble ones, has been recommended [75]. However, these rules were described for pure RTILs. In fact, mixtures of RTILs and organic solvents have been reported to increase the catalytic activity, stability and enantioselectivity of enzymes compared to the single RTIL, probably by reducing the viscosity of the RTIL and diminishing mass-transfer limitations [75]; on the other hand, the proportion and the nature of the organic cosolvent is usually crucial to reach good activity and selectivity (see [75] and references cited therein). Varela et al. [110] collected some data on theoretical studies of mixtures of RTILs and alcohols, concluding that molecular dynamics simulations of the solvation of alcohols in RTILs may resemble water behavior. Thus, the different regions of the bulk RTIL can interact with the analogous (polar or apolar) parts of the solute molecules, and this fact is pivotal for understanding both the mesomorphic structure of the mixtures as well as their dynamics, following a pattern termed “nanostructured solvation” [110]. However, theoretical studies describing the effect of RTIL/organic solvent mixtures on the structure of enzymes are still missing.

Particularly, the use of an apolar organic solvent (toluene) has been reported to increase BTL2 rigidity, as deduced from molecular dynamics simulations at temperatures as high as 450°K (176.85 °C) [72], without observing any tendency for the lid to open. These same authors described that either inserting a thin layer of water around the enzyme or promoting a single point mutation (G116P)

would be required for retaining activity in acyl-transfer processes [72]. Additionally, another very recent study confirmed the reduced flexibility of BTL2 in nonpolar organic solvents, using molecular dynamics on toluene and cyclohexane, and thus confirming the enhancement of thermostability of BTL2 in the presence of these type of solvents [38]. These theoretical studies would support our results obtained using *isooctane* (Figure 1 and Table 1), where we observed how increasing the reaction temperature up to 90 °C promoted a moderate rise in the reaction rate, but with no enantioselectivity, as the lid should not open (the only water present in the medium would be that one retained in the enzymatic liophilizate, not enough to reach a proper concentration) and therefore not upholding the lid flexibility required for the proper enzymatic enantiodiscrimination [111,112].

It has been also described that polar solvents (water and short-chain alcohols) lead to enhanced fluctuation of BTL2's lid at low temperatures, but surprisingly the open conformation turned out to be more stable in EtOH than in water or MeOH [38]. Thus, considering the beneficial effect of EtOH on BTL2, we decide to check the catalytic performance in mixtures between different RTILs and EtOH. As pointed out in Section 4.2, EtOH was used in a high molar excess compared to the starting substrate (3.42 M EtOH versus 60 mM for (*R,S*)-1), but if we consider the molar fraction of the RTIL and EtOH, the situation is different, as indicated in Table 3.

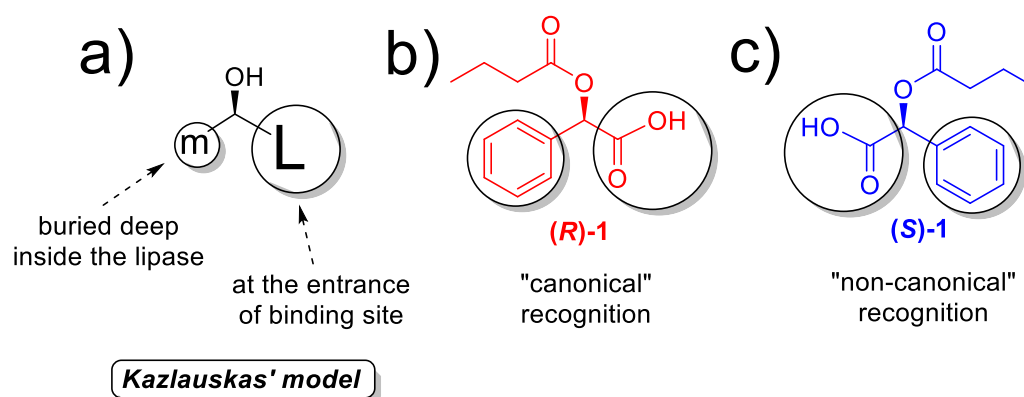
Table 3. Composition of the different reaction mixtures EtOH/RTIL (1 mL/4 mL, V/V).

RTIL	MW ¹ (g/mol)	Density ¹ (g/mL)	[RTIL], M	[EtOH], M	Molar Fraction X_{RTIL}
BMIMBF ₄	226.02	1.21	4.28	3.42	0.56
BMIMPF ₆	284.19	1.38	3.89	3.42	0.53
EMIMBF ₄	197.97	1.29	5.22	3.42	0.60
EMIMPF ₆	256.13	1.48	4.62	3.42	0.57

¹ data from SciFinder database.

As can be seen from Table 3, the molar composition of the reaction mixture is not exactly the same, because of the differences in the molecular weight and density of the four RTILs, although an average value of (0.56 ± 0.04) for X_{RTIL} can be taken as an average.

The most hydrophobic RTIL, water-insoluble BMIMPF₆, is definitively not the best option for the ethanolysis of (*R,S*)-1, as shown in Figure 3, neither at 90 nor at 120 °C; in fact, the initial rate in the generation of (*S*)-2 at 90 °C is not the highest, although enantioselectivity is perfect ($E > 200$) up to 24 h. At 120 °C, an inversion in the stereobias at 120 °C was observed, but only a maximum of 6% conversion is detected for (*R*)-2. Looking at the literature, (*R*)-1 is the recognized enantiomer in the hydrolysis of (*R,S*)-1 by wild-type BTL2 [56], as well as by some immobilized preparation of this enzyme [45], so that the “canonical” recognition, as predicted by the well-known Kazlauskas' rule (Scheme 2a), based on the relative size of substituents around the stereocenter [113] would be that one depicted in Scheme 2b.



Scheme 2. (a) Kazlauskas' rule; (b) "canonical" recognition of (*R*)-1 enantiomer; (c) "noncanonical" recognition of (*S*)-1 enantiomer.

Actually, the large (L) binding pockets is located at the entrance of binding site, while the other medium (m) pocket is buried deep inside the lipase; thus, this would mean that the phenyl ring of the (*R*)-substrate would be the one interacting with the cavity inside the 3D structure of BTL2 in the canonical recognition pattern. This interaction could be caused by a π -stacking of the phenyl moiety of (*R*)-1 with Phe17, a residue which changes its conformation in the open structure and allows the access of the substrate to the catalytic serine [37]; a similar interaction has been proposed for other aromatic substrates with lipases [114,115]. However, using BMIMPF₆ at 90 °C, the non-Kazlauskas recognition (Scheme 2c) is majoritarian, while increasing temperature up to 120 °C, an alteration of the enantioselectivity is observed, but this could be attributed to an enzyme inactivation, as long as the activity dropped dramatically.

Changing from BMIMPF₆ (Figure 3) to BMIMBF₄ (Figure 2), the resolution become faster at 90 °C, (Table 2), but even better at 120 °C, when the inversion of the canonical recognition is absolute, up to the point that no (*S*)-2 is detected at all, and the (*S*)-selection is maintained until the reaction ends (after 12 h, Figure 2b). Filice et al. [116] described that the BF₄ does not cause negative effects on BTL2 in aqueous media, as it happens with other lipases. However, the change of the canonical (Scheme 2b) recognition to the non-Kazlauskas pattern (Scheme 2c) upon heating at 120 °C may be caused by many possible factors. Indeed, a different hydrogen bonding arrangement is one of the reported reason for changing the enantioselection of lipases [117,118], and it is well known that the anionic component of a RTIL is the main responsible of establishing the hydrogen-bonding network with the enzyme [75]; anyhow, this assumption would demand a systematic molecular dynamics study, out of the scope of this paper. In this sense, some preliminary data (not published) obtained in our group have revealed that the half-life of an hydrogen bond between BTL2 and BMIMBF₄ at 120 °C is twice that one in water, partially reinforcing our hypotheses.

On the other hand, the use of more hydrophilic 1-ethyl-3-methyl imidazolium (EMIM) cation has been recommended for BTL2 [116]. Similarly, for other lipases it has been also shown how the shorter the alkyl chain in the cationic imidazolium, the higher the activity [119], while Filice et al. recommended the use of hexafluorophosphate (PF₆⁻) combined with EMIM [116]. In fact, by looking at the progress curves obtained in the ethanolysis of (*R,S*)-1 using EtOH/EMIMPF₆ and depicted in Figure 5a (90 °C) and Figure 5b (120 °C), the kinetic resolutions are quite good, although better at 90 °C. In any case, it is noteworthy to observe how BTL2 is totally enantioselective under these reaction conditions, as no traces of the "canonical" (*R*)-2 isomer were detected.

When using EtOH/EMIMBF₄ at 90 °C (Figure 4a), the situation is quite similar to that obtained with BMIMBF₄ (Figure 2a) or BMIMPF₆ (Figure 3a); nevertheless, the kinetic resolution is much better when using EtOH/EMIMBF₄ at 120° (Figure 4b), as in only 2.5 h a total 50% conversion in (*S*)-2 is obtained, and again no traces of the (*R*)-antipode are formed. To our knowledge, this is the best and faster lipase-catalyzed kinetic resolution ever reported for enantiomers of mandelic acid.

Thus, the best results, both in terms of reaction rate and enantioselectivity, are those obtained using this RTIL formed by the most hydrophilic cation and the most hydrophilic anion, at 120 °C. Once again, we cannot propose a certain reason to explain this behavior, as that was not the purpose of this manuscript. According to the theoretical studies from Shehata et al. [53], the presence of EtOH in the reaction medium would allow the fluctuation of the lid to allow the active site to get exposed and is very compatible with BTL2 stability, as for sure EMIMBF₄ has also demonstrated to be.

4. Materials

Lipase from *Geobacillus thermocatenulatus* was a kind gift of the Biochemistry, Genetics and Immunology Department of the Universidad de Vigo, Spain. All solvents of the highest purity commercially available and used without purification were purchased from Sigma-Aldrich-Fluka, (Barcelona, Spain). All other chemicals and RTILs (1-butyl-3-methyl imidazolium tetrafluoroborate (BMIMBF₄), 1-butyl-3-methyl imidazolium hexafluorophosphate (BMIMPF₆), 1-ethyl-3-methyl imidazolium tetrafluoroborate (EMIMBF₄) and 1-ethyl-3-methyl imidazolium hexafluorophosphate (EMIMPF₆) were purchased also from Sigma-Aldrich-Fluka (Barcelona, Spain).

4.1. Synthesis of (R,S) 2-(Butyryloxy)-2-phenylacetic Acid

Twenty mmol of mandelic acid in 200 mL of diethyl ether were added to 2.88 mL triethylamine (20 mmol). Subsequently, a solution of 2.131 mL (20 mmol) butyryl chloride in 100 mL ethyl ether was dropped. The reaction was carried out in a flask at 25 °C for approximately four hours, giving a yield of 50%. Reaction progress was followed by HPLC, ¹H-NMR and ¹³C-NMR (Bruker AC-250 (¹H), 63 MHz (¹³C), Bruker Corporation, Billerica, MA, USA).

Simply by adding water, the unreacted acid could be separated from the ester, which remained in the organic phase. Acid was removed performing successive washing with water. Subsequently, organic phase was dried with anhydrous sodium sulfate and the remaining ether was removed using rotary evaporator. Successive extraction with diethyl ether, allowed the isolation of 7 g of yellowish oil as a final product ((R, S) 2-butanoyloxy phenyl acetic). spectroscopic data were according to those previously reported in literature [120].

4.2. Resolution of 2-(Butyryloxy)-2-phenylacetic Acid by Alcoholysis Reaction

Reactions were carried out in closed glass vials and the temperature of the experiments varied between 40 and 120 °C. In the case of *isooctane*, temperatures of 40, 70 and 90 °C were used, whereas ionic liquids were tested at 90 and 120 °C. To maintain the temperature fixed, a thermostat-equipped bath oil was used for several days. The reaction mixture included: an organic solvent or RTIL (4 mL), 2-(butyryloxy)-2-phenylacetic acid (60 mM) and ethanol (1 mL), assuring a molar excess of alcohol versus the organic acid. Then, the enzyme (4 mg solid/mL) was added. In order to ensure that reaction is due only to the lipase, a reaction test without lipase was carried out. As a consequence of the employment of high temperatures, the vials were rapidly cooled down for sampling previously to the opening to avoid any evaporation of the alcohol; thus, aliquots of 100 µL were taken at different times. As RTILs cannot be directly injected into the HPLC (Constrametric 4100 pump, UV detector Spectromonitor 5000, LDC Analytical, Spain), the samples were extracted with 1 mL of diethyl ether and the solvent evaporated at room temperature; subsequently, they were re-diluted with 400 µL hexane/2-propanol (1:1) (*v/v*) and filtered using syringe filters (Millex-GV (PVDF), 0.22 µm pore size). HPLC analysis was performed using a Chiracel OD (20 µm (250 × 4.6 mm) chiral column, a mobile phase composed by *n*-hexane/2-propanol/trifluoroacetic acid (90/9/1), a 0.8 mL/min flux and a wavelength of 254 nm. Peak assignation was determined using pure compounds as standards.

5. Conclusions

Although thermophilic enzymes can efficiently work at very high temperature, they are more stereoselective when used at temperature below their optimal one, as they are more rigid under

those reaction conditions. Consequently, finding a thermophilic enzyme capable to retain its activity and stereodiscrimination capability at high temperature would lead to very fast and stereoselective processes. In this paper, we have shown how binary mixtures of EtOH and room temperature ionic liquids (RTILs) are an excellent reaction media for the enantioselective kinetic resolution (KR) of racemic 2-(butyryloxy)-2-phenylacetic acid via ethanolysis catalyzed by lipase-form *Geobacillus thermocatenulatus* (BTL2) at very high reaction temperatures (120°). Thus, the KR carried out using an EtOH/BMIMBF₄ at 120 °C furnished (R)-mandelic acid as the only reaction product (E > 200) at very short reaction time (12 h), while by changing the composition of the cationic moiety of the RTIL, then using EtOH/EMIMBF₄ at the same temperature of 120 °C, an ever faster (2.5 h reaction time) and completely enantioselective KR led to enantiopure (S)-mandelic acid. This is the faster described KR for this substrate. The previously reported beneficial effect of EtOH on BTL2, stabilizing its open active conformation even at extreme temperatures, as deduced from molecular dynamics, is supporting our results; on the other hand, the establishment of very strong hydrogen bonds between the enzyme and the RTIL could be the responsible for the observed thermostability.

Author Contributions: Experimental data, J.R.-M., O.K.; writing—original draft preparation, J.R.-M., O.K.; writing—review and editing, A.R.A., J.M.S.-M. Both corresponding authors have similarly contributed to the final version of the manuscript. All authors have read and agreed to the published version of the manuscript.

Funding: This research was partially funded by Projects CTQ2017-86170-R (MINECO-Spanish Government) and PR87/19-22676 (Banco de Santander-Complutense Research Projects).

Conflicts of Interest: The authors declare no conflict of interest.

References

1. Wiltschi, B.; Cernava, T.; Dennig, A.; Casas, M.G.; Geier, M.; Gruber, S.; Haberbauer, M.; Heidinger, P.; Acero, E.H.; Kratzer, R.; et al. Enzymes revolutionize the bioproduction of value-added compounds: From enzyme discovery to special applications. *Biotechnol. Adv.* **2020**, *40*, 51. [[CrossRef](#)] [[PubMed](#)]
2. Woodley, J.M. New frontiers in biocatalysis for sustainable synthesis. *Curr. Opin. Green Sustain. Chem.* **2020**, *21*, 22–26. [[CrossRef](#)]
3. Huang, X.; Cao, M.; Zhao, H. Integrating biocatalysis with chemocatalysis for selective transformations. *Curr. Opin. Chem. Biol.* **2020**, *55*, 161–170. [[CrossRef](#)] [[PubMed](#)]
4. Li, J.; Amatuni, A.; Renata, H. Recent advances in the chemoenzymatic synthesis of bioactive natural products. *Curr. Opin. Chem. Biol.* **2020**, *55*, 111–118. [[CrossRef](#)] [[PubMed](#)]
5. Sheldon, R.A.A.; Brady, D.; Bode, M.L.L. The Hitchhiker's guide to biocatalysis: Recent advances in the use of enzymes in organic synthesis. *Chem. Sci.* **2020**, *11*, 2587–2605. [[CrossRef](#)]
6. Sandoval, B.A.; Hyster, T.K. Emerging strategies for expanding the toolbox of enzymes in biocatalysis. *Curr. Opin. Chem. Biol.* **2020**, *55*, 45–51. [[CrossRef](#)]
7. Chapman, J.; Ismail, A.; Dinu, C. Industrial Applications of Enzymes: Recent Advances, Techniques, and Outlooks. *Catalysts* **2018**, *8*, 238. [[CrossRef](#)]
8. de Gonzalo, G.; Domínguez de María, P. *Biocatalysis: An Industrial Perspective*; Royal Society of Chemistry: London, UK, 2018. [[CrossRef](#)]
9. Woodley, J.M. Accelerating the implementation of biocatalysis in industry. *Appl. Microbiol. Biotechnol.* **2019**, *103*, 4733–4739. [[CrossRef](#)]
10. Hughes, G.; Lewis, J.C. Introduction: Biocatalysis in Industry. *Chem. Rev.* **2018**, *118*, 1–3. [[CrossRef](#)]
11. Domínguez de María, P.; de Gonzalo, G.; Alcántara, A.R. Biocatalysis as useful tool in asymmetric synthesis: An assessment of recently granted patents (2014–2019). *Catalysts* **2019**, *9*, 802. [[CrossRef](#)]
12. Alcántara, A.R. Biotransformations in Drug Synthesis: A Green and Powerful Tool for Medicinal Chemistry. *J. Med. Chem. Drug. Des.* **2018**, *1*, 1–7. [[CrossRef](#)]
13. Hoyos, P.; Pace, V.; Alcántara, A.R. Chiral Building Blocks for Drugs Synthesis via Biotransformations. In *Asymmetric Synthesis of Drugs and Natural Products*; Nag, A., Ed.; CRC Press: Boca Raton, FL, USA, 2018; pp. 346–448.
14. Alcántara, A.R. Biocatalysis and Pharmaceuticals: A Smart Tool for Sustainable Development. *Catalysts* **2019**, *9*, 792. [[CrossRef](#)]

15. Truppo, M.D. Biocatalysis in the Pharmaceutical Industry: The Need for Speed. *ACS Med. Chem. Lett.* **2017**, *8*, 476–480. [[CrossRef](#)] [[PubMed](#)]
16. Rosenthal, K.; Lutz, S. Recent developments and challenges of biocatalytic processes in the pharmaceutical industry. *Curr. Opin. Green Sustain. Chem.* **2018**, *11*, 58–64. [[CrossRef](#)]
17. Lalor, F.; Fitzpatrick, J.; Sage, C.; Byrne, E. Sustainability in the biopharmaceutical industry: Seeking a holistic perspective. *Biotechnol. Adv.* **2019**, *37*, 698–703. [[CrossRef](#)] [[PubMed](#)]
18. Sheldon, R.A.; Woodley, J.M. Role of Biocatalysis in Sustainable Chemistry. *Chem. Rev.* **2018**, *118*, 801–838. [[CrossRef](#)] [[PubMed](#)]
19. Sheldon, R.A.; Brady, D. Broadening the Scope of Biocatalysis in Sustainable Organic Synthesis. *ChemSusChem* **2019**, *12*, 2859–2881. [[CrossRef](#)]
20. Kumar, S.; Dang, A.K.; Shukla, P.; Baishya, D.; Khare, S.K. Thermozyms: Adaptive strategies and tools for their biotechnological applications. *Bioresour. Technol.* **2019**, *278*, 372–382. [[CrossRef](#)]
21. Han, H.W.; Ling, Z.M.; Khan, A.; Virk, A.K.; Kulshrestha, S.; Li, X.K. Improvements of thermophilic enzymes: From genetic modifications to applications. *Bioresour. Technol.* **2019**, *279*, 350–361. [[CrossRef](#)]
22. González-Siso, M.-I. Editorial for the Special Issue: Thermophiles and Thermozyms. *Microorganisms* **2019**, *7*, 62. [[CrossRef](#)]
23. Atalah, J.; Caceres-Moreno, P.; Espina, G.; Blamey, J.M. Thermophiles and the applications of their enzymes as new biocatalysts. *Bioresour. Technol.* **2019**, *280*, 478–488. [[CrossRef](#)] [[PubMed](#)]
24. Hait, S.; Mallik, S.; Basu, S.; Kundu, S. Finding the generalized molecular principles of protein thermal stability. *Proteins* **2020**, *88*, 788–808. [[CrossRef](#)] [[PubMed](#)]
25. Liszka, M.J.; Clark, M.E.; Schneider, E.; Clark, D.S. Nature Versus Nurture: Developing Enzymes That Function Under Extreme Conditions. In *Annual Review of Chemical and Biomolecular Engineering*; Prausnitz, J.M., Ed.; Annual Reviews: Palo Alto, CA, USA, 2012; Volume 3, pp. 77–102.
26. Stepankova, V.; Bidmanova, S.; Koudelakova, T.; Prokop, Z.; Chaloupkova, R.; Damborsky, J. Strategies for Stabilization of Enzymes in Organic Solvents. *ACS Catal.* **2013**, *3*, 2823–2836. [[CrossRef](#)]
27. Dumorne, K.; Cordova, D.C.; Astorga-Elo, M.; Renganathan, P. Extremozymes: A Potential Source for Industrial Applications. *J. Microbiol. Biotechnol.* **2017**, *27*, 649–659. [[CrossRef](#)] [[PubMed](#)]
28. Filho, D.G.; Silva, A.G.; Guidini, C.Z. Lipases: Sources, immobilization methods, and industrial applications. *Appl. Microb. Biotechnol.* **2019**, *103*, 7399–7423. [[CrossRef](#)] [[PubMed](#)]
29. Daiha, K.D.; Angeli, R.; de Oliveira, S.D.; Almeida, R.V. Are lipases still important biocatalysts? A study of scientific publications and patents for technological forecasting. *PLoS ONE* **2019**, *10*, 20. [[CrossRef](#)] [[PubMed](#)]
30. Dwivedee, B.P.; Soni, S.; Sharma, M.; Bhaumik, J.; Laha, J.K.; Banerjee, U.C. Promiscuity of lipase-catalyzed reactions for organic synthesis: A recent update. *ChemistrySelect* **2018**, *3*, 2441–2466. [[CrossRef](#)]
31. Sarmah, N.; Revathi, D.; Sheelu, G.; Rani, K.Y.; Sridhar, S.; Mehtab, V.; Sumana, C. Recent advances on sources and industrial applications of lipases. *Biotechnol. Prog.* **2018**, *34*, 5–28. [[CrossRef](#)]
32. Priyanka, P.; Tan, Y.Q.; Kinsella, G.K.; Henahan, G.T.; Ryan, B.J. Solvent stable microbial lipases: Current understanding and biotechnological applications. *Biotechnol. Lett.* **2019**, *41*, 203–220. [[CrossRef](#)] [[PubMed](#)]
33. Kumar, A.; Dhar, K.; Kanwar, S.S.; Arora, P.K. Lipase catalysis in organic solvents: Advantages and applications. *Biol. Proced. Online* **2016**, *18*, 2. [[CrossRef](#)] [[PubMed](#)]
34. Mohtashami, M.; Fooladi, J.; Haddad-Mashadrizesh, A.; Housaindokht, M.R.; Monhemi, H. Molecular mechanism of enzyme tolerance against organic solvents: Insights from molecular dynamics simulation. *Int. J. Biol. Macromol.* **2019**, *122*, 914–923. [[CrossRef](#)] [[PubMed](#)]
35. Elleuche, S.; Schroder, C.; Antranikian, G. Lipolytic extremozymes from psychro- and (hyper-)thermophilic prokaryotes and their potential for industrial applications. In *Biotechnology of Extremophiles: Advances and Challenges*; Rampelotto, P.H., Ed.; Springer International Publishing Ag: Cham, Switzerland, 2016; Volume 1, pp. 351–374.
36. Lajis, A.F.B. Realm of Thermoalkaline Lipases in Bioprocess Commodities. *J. Lipids* **2018**, *2018*, 5659683. [[CrossRef](#)]
37. Carrasco-Lopez, C.; Godoy, C.; de las Rivas, B.; Fernandez-Lorente, G.; Palomo, J.M.; Guisan, J.M.; Fernandez-Lafuente, R.; Martinez-Ripoll, M.; Hermoso, J.A. Activation of bacterial thermoalkalophilic lipases is spurred by dramatic structural rearrangements. *J. Biol. Chem.* **2009**, *284*, 4365–4372. [[CrossRef](#)] [[PubMed](#)]

38. Shehata, M.; Timucin, E.; Venturini, A.; Sezerman, O.U. Understanding thermal and organic solvent stability of thermoalkalophilic lipases: Insights from computational predictions and experiments. *J. Mol. Model.* **2020**, *26*, 1–12. [[CrossRef](#)]
39. Nazina, T.N.; Tourova, T.P.; Poltarau, A.B.; Novikova, E.V.; Grigoryan, A.A.; Ivanova, A.E.; Lysenko, A.M.; Petrunyaka, V.V.; Osipov, G.A.; Belyaev, S.S.; et al. Taxonomic study of aerobic thermophilic bacilli: Descriptions of *Geobacillus subterraneus* gen. nov., sp nov and *Geobacillus uzenensis* sp nov from petroleum reservoirs and transfer of *Bacillus stearothermophilus*, *Bacillus thermocatenulatus*, *Bacillus thermoleovorans*, *Bacillus kaustophilus*, *Bacillus thermoglucosidasius* and *Bacillus thermodenitrificans* to *Geobacillus* as the new combinations *G. stearothermophilus*, *G. thermocatenulatus*, *G. thermoleovorans*, *G. kaustophilus*, *G. thermoglucosidasius* and *G. thermodenitrificans*. *Int. J. Syst. Evol. Microbiol.* **2001**, *51*, 433–446. [[CrossRef](#)]
40. Schmidt-Dannert, C.; Sztajer, H.; Stocklein, W.; Menge, U.; Schmid, R.D. Screening, purification and properties of a thermophilic lipase from *Bacillus thermocatenulatus*. *Biochim. Biophys. Acta Lipids Lipid Metab.* **1994**, *1214*, 43–53. [[CrossRef](#)]
41. Schmidt-Dannert, C.; Rua, M.L.; Schmid, R.D. *Bacillus thermocatenulatus* lipase: A thermoalkalophilic lipase with interesting properties. *Biochem. Soc. Trans.* **1997**, *25*, 178–182. [[CrossRef](#)]
42. Schmidt-Dannert, C.; Rua, M.L.; Atomi, H.; Schmid, R.D. Thermoalkalophilic lipase of *Bacillus thermocatenulatus*. 1. Molecular cloning, nucleotide sequence, purification and some properties. *Biochim. Biophys. Acta Lipids Lipid Metab.* **1996**, *1301*, 105–114. [[CrossRef](#)]
43. Carrasco-Lopez, C.; Godoy, C.; de las Rivas, B.; Fernandez-Lorente, G.; Palomo, J.M.; Guisan, J.M.; Fernandez-Lafuente, R.; Martinez-Ripoll, M.; Hermoso, J.A. Crystallization and preliminary X-ray diffraction studies of the BTL2 lipase from the extremophilic microorganism *Bacillus thermocatenulatus*. *Acta Crystallogr. F Struct. Biol. Commun.* **2008**, *64*, 1043–1045. [[CrossRef](#)]
44. Liu, A.M.F.; Somers, N.A.; Kazlauskas, R.J.; Brush, T.S.; Zocher, F.; Enzelberger, M.M.; Bornscheuer, U.T.; Horsman, G.P.; Mezzetti, A.; Schmidt-Dannert, C.; et al. Mapping the substrate selectivity of new hydrolases using colorimetric screening: Lipases from *Bacillus thermocatenulatus* and *Ophiostoma piliferum*, esterases from *Pseudomonas fluorescens* and *Streptomyces diastatochromogenes*. *Tetrahedron Asymmetry* **2001**, *12*, 545–556. [[CrossRef](#)]
45. Palomo, J.M.; Fernandez-Lorente, G.; Rua, M.L.; Guisan, J.M.; Fernandez-Lafuente, R. Evaluation of the lipase from *Bacillus thermocatenulatus* as an enantioselective biocatalyst. *Tetrahedron Asymmetry* **2003**, *14*, 3679–3687. [[CrossRef](#)]
46. Palomo, J.M.; Ortiz, C.; Fuentes, M.; Fernandez-Lorente, G.; Guisan, J.M.; Fernandez-Lafuente, R. Use of immobilized lipases for lipase purification via specific lipase-lipase interactions. *J. Chromatogr. A* **2004**, *1038*, 267–273. [[CrossRef](#)] [[PubMed](#)]
47. Palomo, J.M.; Segura, R.L.; Fernandez-Lorente, G.; Pernas, M.; Rua, M.L.; Guisan, J.M.; Fernandez-Lafuente, R. Purification, immobilization, and stabilization of a lipase from *Bacillus thermocatenulatus* by interfacial adsorption on hydrophobic supports. *Biotechnol. Prog.* **2004**, *20*, 630–635. [[CrossRef](#)]
48. Fernandez-Lorente, G.; Cabrera, Z.; Godoy, C.; Fernandez-Lafuente, R.; Palomo, J.M.; Guisan, J.M. Interfacially activated lipases against hydrophobic supports: Effect of the support nature on the biocatalytic properties. *Process. Biochem.* **2008**, *43*, 1061–1067. [[CrossRef](#)]
49. Fernandez-Lorente, G.; Godoy, C.A.; Mendes, A.A.; Lopez-Gallego, F.; Grazu, V.; de las Rivas, B.; Palomo, J.M.; Hermoso, J.; Fernandez-Lafuente, R.; Guisan, J.M. Solid-phase chemical amination of a lipase from *Bacillus thermocatenulatus* to improve its stabilization via covalent immobilization on highly activated glyoxyl-agarose. *Biomacromolecules* **2008**, *9*, 2553–2561. [[CrossRef](#)]
50. Bolivar, J.M.; Mateo, C.; Godoy, C.; Pessela, B.C.C.; Rodrigues, D.S.; Giordano, R.L.C.; Fernandez-Lafuente, R.; Guisan, J.M. The co-operative effect of physical and covalent protein adsorption on heterofunctional supports. *Process. Biochem.* **2009**, *44*, 757–763. [[CrossRef](#)]
51. Godoy, C.A.; de las Rivas, B.; Filice, M.; Fernandez-Lorente, G.; Guisan, J.M.; Palomo, J.M. Enhanced activity of an immobilized lipase promoted by site-directed chemical modification with polymers. *Process. Biochem.* **2010**, *45*, 534–541. [[CrossRef](#)]
52. Godoy, C.A.; de las Rivas, B.; Bezbradica, D.; Bolivar, J.M.; Lopez-Gallego, F.; Fernandez-Lorente, G.; Guisan, J.M. Reactivation of a thermostable lipase by solid phase unfolding/refolding Effect of cysteine residues on refolding efficiency. *Enzyme Microb. Technol.* **2011**, *49*, 388–394. [[CrossRef](#)] [[PubMed](#)]

53. Godoy, C.A.; de las Rivas, B.; Grazu, V.; Montes, T.; Manuel Guisan, J.; Lopez-Gallego, F. Glyoxyl-Disulfide Agarose: A Tailor-Made Support for Site-Directed Rigidification of Proteins. *Biomacromolecules* **2011**, *12*, 1800–1809. [[CrossRef](#)] [[PubMed](#)]
54. Godoy, C.A.; Fernandez-Lorente, G.; de las Rivas, B.; Filice, M.; Guisan, J.M.; Palomo, J.M. Medium engineering on modified *Geobacillus thermocatenulatus* lipase to prepare highly active catalysts. *J. Mol. Catal. B Enzym.* **2011**, *70*, 144–148. [[CrossRef](#)]
55. Lopez-Gallego, F.; Abian, O.; Manuel Guisan, J. Altering the Interfacial Activation Mechanism of a Lipase by Solid-Phase Selective Chemical Modification. *Biochemistry* **2012**, *51*, 7028–7036. [[CrossRef](#)] [[PubMed](#)]
56. Godoy, C.A.; Romero, O.; de la Rivas, B.; Mateo, C.; Fernandez-Lorente, G.; Guisan, J.M.; Palomo, J.M. Changes on enantioselectivity of a genetically modified thermophilic lipase by site-directed oriented immobilization. *J. Mol. Catal. B Enzym.* **2013**, *87*, 121–127. [[CrossRef](#)]
57. Marciello, M.; Bolivar, J.M.; Filice, M.; Mateo, C.; Guisan, J.M. Preparation of Lipase-Coated, Stabilized, Hydrophobic Magnetic Particles for Reversible Conjugation of Biomacromolecules. *Biomacromolecules* **2013**, *14*, 602–607. [[CrossRef](#)]
58. Bautista-Barrufet, A.; Lopez-Gallego, F.; Rojas-Cervellera, V.; Rovira, C.; Pericas, M.A.; Guisan, J.M.; Gorostiza, P. Optical Control of Enzyme Enantioselectivity in Solid Phase. *ACS Catal.* **2014**, *4*, 1004–1009. [[CrossRef](#)]
59. Mendes, A.A.; Oliveira, P.C.; Velez, A.M.; Giordano, R.C.; Giordano, R.d.L.C.; de Castro, H.F. Evaluation of immobilized lipases on poly-hydroxybutyrate beads to catalyze biodiesel synthesis. *Int. J. Biol. Macromol.* **2012**, *50*, 503–511. [[CrossRef](#)]
60. Herranz, S.; Marciello, M.; Olea, D.; Hernandez, M.; Domingo, C.; Velez, M.; Gheber, L.A.; Guisan, J.M.; Moreno-Bondi, M.C. Dextran-Lipase Conjugates as Tools for Low Molecular Weight Ligand Immobilization in Microarray Development. *Anal. Chem.* **2013**, *85*, 7060–7068. [[CrossRef](#)]
61. Guajardo, N.; Bernal, C.; Wilson, L.; Cabrera, Z. Asymmetric hydrolysis of dimethyl-3-phenylglutarate in sequential batch reactor operation catalysed by immobilized *Geobacillus thermocatenulatus* lipase. *Catal. Today* **2015**, *255*, 21–26. [[CrossRef](#)]
62. Godoy, C.A. New Strategy for the Immobilization of Lipases on Glyoxyl-Agarose Supports: Production of Robust Biocatalysts for Natural Oil Transformation. *Int. J. Mol. Sci.* **2017**, *18*, 2130. [[CrossRef](#)]
63. Lopez-Tejedor, D.; de las Rivas, B.; Palomo, J.M. Ultra-Small Pd(0) Nanoparticles into a Designed Semisynthetic Lipase: An Efficient and Recyclable Heterogeneous Biohybrid Catalyst for the Heck Reaction under Mild Conditions. *Molecules* **2018**, *23*, 2358. [[CrossRef](#)]
64. Romero, O.; de las Rivas, B.; Lopez-Tejedor, D.; Palomo, J.M. Effect of Site-Specific Peptide-Tag Labeling on the Biocatalytic Properties of Thermoalkalophilic Lipase from *Geobacillus thermocatenulatus*. *ChemBioChem* **2018**, *19*, 369–378. [[CrossRef](#)] [[PubMed](#)]
65. Moreno-Perez, S.; Fernandez-Lorente, G.; Romero, O.; Guisan, J.M.; Lopez-Gallego, F. Fabrication of heterogeneous biocatalyst tethering artificial prosthetic groups to obtain omega-3-fatty acids by selective hydrolysis of fish oils. *RSC Adv.* **2016**, *6*, 97659–97663. [[CrossRef](#)]
66. Cowan, D.A.; Fernandez-Lafuente, R. Enhancing the functional properties of thermophilic enzymes by chemical modification and immobilization. *Enzyme Microb. Technol.* **2011**, *49*, 326–346. [[CrossRef](#)]
67. Godoy, C.A.; de las Rivas, B.; Guisan, J.M. Site-directing an intense multipoint covalent attachment (MCA) of mutants of the *Geobacillus thermocatenulatus* lipase 2 (BTL2): Genetic and chemical amination plus immobilization on a tailor-made support. *Process. Biochem.* **2014**, *49*, 1324–1331. [[CrossRef](#)]
68. Kajiwara, S.; Yamada, R.; Matsumoto, T.; Ogino, H. N-linked glycosylation of thermostable lipase from *Bacillus thermocatenulatus* to improve organic solvent stability. *Enzyme Microb. Technol.* **2020**, *132*. [[CrossRef](#)] [[PubMed](#)]
69. Godoy, C.A.; Klett, J.; Di Geronimo, B.; Hermoso, J.A.; Guisan, J.M.; Carrasco-Lopez, C. Disulfide Engineered Lipase to Enhance the Catalytic Activity: A Structure-Based Approach on BTL2. *Int. J. Mol. Sci.* **2019**, *20*, 5245. [[CrossRef](#)] [[PubMed](#)]
70. Karimi, E.; Karkhane, A.A.; Yakhchali, B.; Shamsara, M.; Aminzadeh, S.; Torktaiz, I.; Hosseini, M.; Safari, Z. Study of the effect of F17A mutation on characteristics of *Bacillus thermocatenulatus* lipase expressed in *Pichia pastoris* using *in silico* and experimental methods. *Biotech. Appl. Biochem.* **2014**, *61*, 264–273. [[CrossRef](#)]

71. Goodarzi, N.; Karkhane, A.A.; Mirlohi, A.; Tabandeh, F.; Torktas, I.; Aminzadeh, S.; Yakhchali, B.; Shamsara, M.; Ghafouri, M.A.-S. Protein engineering of *Bacillus thermocatenulatus* lipase via deletion of the alpha 5 helix. *Appl. Biochem. Biotech.* **2014**, *174*, 339–351. [[CrossRef](#)]
72. Yenenler, A.; Venturini, A.; Burduroglu, H.C.; Sezerman, O.U. Investigating the structural properties of the active conformation BTL2 of a lipase from *Geobacillus thermocatenulatus* in toluene using molecular dynamic simulations and engineering BTL2 via in-silico mutation. *J. Mol. Model.* **2018**, *24*, 13. [[CrossRef](#)]
73. Yukselen, O.; Timucin, E.; Sezerman, U. Predicting the impact of mutations on the specific activity of *Bacillus thermocatenulatus* lipase using a combined approach of docking and molecular dynamics. *J. Mol. Recognit.* **2016**, *29*, 466–475. [[CrossRef](#)]
74. Khaleghinejad, S.H.; Motaleb, G.; Karkhane, A.A.; Aminzadeh, S.; Yakhchali, B. Study the effect of F17S mutation on the chimeric *Bacillus thermocatenulatus* lipase. *J. Genet. Eng. Biotechnol.* **2016**, *14*, 83–89. [[CrossRef](#)]
75. Wang, S.H.; Meng, X.H.; Zhou, H.; Liu, Y.; Secundo, F.; Liu, Y. Enzyme stability and activity in non-aqueous reaction systems: A mini review. *Catalysts* **2016**, *6*, 32. [[CrossRef](#)]
76. Elgharbawy, A.A.; Riyadi, F.A.; Alam, M.Z.; Moniruzzaman, M. Ionic liquids as a potential solvent for lipase-catalysed reactions: A review. *J. Mol. Liq.* **2018**, *251*, 150–166. [[CrossRef](#)]
77. Elgharbawy, A.A.M.; Moniruzzaman, M.; Goto, M. Recent advances of enzymatic reactions in ionic liquids: Part II. *Biochem. Eng. J.* **2020**, *154*, 23. [[CrossRef](#)]
78. Itoh, T. Ionic Liquids as Tool to Improve Enzymatic Organic Synthesis. *Chem. Rev.* **2017**, *117*, 10567–10607. [[CrossRef](#)]
79. de los Rios, A.P.; Irabien, A.; Hollmann, F.; Fernandez, F.J.H. Ionic Liquids: Green Solvents for Chemical Processing. *J. Chem.* **2013**, *2013*, 402172. [[CrossRef](#)]
80. Clarke, C.J.; Tu, W.C.; Levers, O.; Brohl, A.; Hallett, J.P. Green and Sustainable Solvents in Chemical Processes. *Chem. Rev.* **2018**, *118*, 747–800. [[CrossRef](#)]
81. Terreni, M.; Pagani, G.; Ubiali, D.; Fernandez-Lafuente, R.; Mateo, C.; Guisan, J.M. Modulation of penicillin acylase properties via immobilization techniques: One-pot chemoenzymatic synthesis of cephamandole from cephalosporin C. *Bioorg. Med. Chem. Lett.* **2001**, *11*, 2429–2432. [[CrossRef](#)]
82. Furlenmeier, A.; Quitt, P.; Vogler, K.; Lanz, P. 6-Acyl Derivatives of Aminopenicillanic Acid. U.S. Patent US3957758A, 18 May 1976.
83. Su, X.P.; Bhongle, N.N.; Pflum, D.; Butler, H.; Wald, S.A.; Bakale, R.P.; Senanayake, C.H. A large-scale asymmetric synthesis of (S)-cyclohexylphenyl glycolic acid. *Tetrahedron Asymmetry* **2003**, *14*, 3593–3600. [[CrossRef](#)]
84. Glushkov, R.G.; Ovcharova, I.M.; Muratov, M.A.; Kaminka, M.E.; Mashkovsky, M.D. Synthesis and pharmacological activity of new oxyaminoalkylxanthines and dialkylaminoalkylxanthines 1,4-diazepino and pyrazino[1,2,3-g,h] purine derivatives. *Khimiko-Farmatseoticheskii Zhurnal* **1977**, *11*, 30–35.
85. Bousquet, A.; Musolino, A. Hydroxyacetic Ester Derivatives, Namely (R)-methyl 2-(sulfonyloxy)-2-(chlorophenyl)acetates, Preparation Method, and Use as Synthesis Intermediates for Clopidogrel. WO9918110A1, 15 April 1999.
86. Bast, A.; Leurs, R.; Timmerman, H. Cyclandelate as a calcium modulating agent in rat cerebral-cortex. *Drugs* **1987**, *33*, 67–74. [[CrossRef](#)]
87. Gokce, M.; Utku, S.; Gur, S.; Ozkul, A.; Gumus, F. Synthesis, in vitro cytotoxic and antiviral activity of cis-[Pt(R(-) and S(+)-2-alpha-hydroxybenzylbenzimidazole)(2)Cl-2] complexes. *Eur. J. Med. Chem.* **2005**, *40*, 135–141. [[CrossRef](#)]
88. Yamamoto, K.; Fujimatsu, I.; Komatsu, K. Purification and characterization of the nitrilase from *Alcaligenes faecalis* ATCC-8750 responsible for enantioselective hydrolysis of mandelonitrile. *J. Ferment. Bioeng.* **1992**, *73*, 425–430. [[CrossRef](#)]
89. Yamamoto, K.; Oishi, K.; Fujimatsu, I.; Komatsu, K.I. Production of R(-)-mandelic acid from mandelonitrile by *Alcaligenes faecalis* ATCC-8750. *Appl. Environ. Microbiol.* **1991**, *57*, 3028–3032. [[CrossRef](#)]
90. Potala, M.; Dranka, M.; Borowiecki, P. Chemoenzymatic Preparation of Enantiomerically Enriched (R)-(-)-Mandelic Acid Derivatives: Application in the Synthesis of the Active Agent Pemoline. *Eur. J. Org. Chem.* **2017**, *2017*, 2290–2304. [[CrossRef](#)]

91. Arroyo, M.; de la Mata, I.; Garcia, J.L.; Barredo, J.L. *Biocatalysis for Industrial Production of Active Pharmaceutical Ingredients (APIs)*; Academic Press Ltd.: Cambridge, MA, USA; Elsevier Science Ltd.: London, UK, 2017; pp. 451–473. [[CrossRef](#)]
92. Martin, J.R.; Nus, M.; Gago, J.V.S.; Sanchez-Montero, J.M. Selective esterification of phthalic acids in two ionic liquids at high temperatures using a thermostable lipase of *Bacillus thermocatenulatus*: A comparative study. *J. Mol. Catal. B Enzym.* **2008**, *52–53*, 162–167. [[CrossRef](#)]
93. Pizzilli, A.; Zoppi, R.; Hoyos, P.; Gómez, S.; Gatti, F.G.; Hernáiz, M.J.; Alcántara, A.R. First stereoselective acylation of a primary diol possessing a prochiral quaternary center mediated by lipase TL from *Pseudomonas stutzeri*. *Tetrahedron* **2015**, *71*, 9172–9176. [[CrossRef](#)]
94. Chamorro, S.; Sanchez-Montero, J.M.; Alcantara, A.R.; Sinisterra, J.V. Treatment of *Candida rugosa* lipase with short-chain polar organic solvents enhances its hydrolytic and synthetic activities. *Biotechnol. Lett.* **1998**, *20*, 499–505. [[CrossRef](#)]
95. Borreguero, I.; Carvalho, C.M.L.; Cabral, J.M.S.; Sinisterra, J.V.; Alcantara, A.R. Enantioselective properties of *Fusarium solani pisi* cutinase on transesterification of acyclic diols: Activity and stability evaluation. *J. Mol. Catal. B Enzym.* **2001**, *11*, 613–622. [[CrossRef](#)]
96. Chamorro, S.; Alcántara, A.R.; de la Casa, R.M.; Sinisterra, J.V.; Sánchez-Montero, J.M. Small water amounts increase the catalytic behaviour of polar organic solvents pre-treated *Candida rugosa* lipase. *J. Mol. Catal. B Enzym.* **2001**, *11*, 939–947. [[CrossRef](#)]
97. Domínguez de María, P.; Martínez-Alzamora, F.; Moreno, S.P.; Valero, F.; Rúa, M.L.; Sánchez-Montero, J.M.; Sinisterra, J.V.; Alcántara, A.R. Heptyl oleate synthesis as useful tool to discriminate between lipases, proteases and other hydrolases in crude preparations. *Enzyme Microb. Technol.* **2002**, *31*, 283–288. [[CrossRef](#)]
98. Alcántara, A.R.; De María, P.D.; Fernández, M.; Hernaíz, M.J.; Sánchez-Montero, J.M.; Sinisterra, J.V. Resolution of racemic acids, esters and amines by *Candida rugosa* lipase in slightly hydrated organic media. *Food Technol. Biotechnol.* **2004**, *42*, 343–354.
99. Alfonsi, K.; Colberg, J.; Dunn, P.J.; Fevig, T.; Jennings, S.; Johnson, T.A.; Kleine, H.P.; Knight, C.; Nagy, M.A.; Perry, D.A.; et al. Green chemistry tools to influence a medicinal chemistry and research chemistry based organisation. *Green Chem.* **2008**, *10*, 31–36. [[CrossRef](#)]
100. Bardsley, W.G. *SIMFIT—A Computer Package for Simulation, Curve-Fitting and Statistical-Analysis using Life-Science Models*; Plenum Press Div. Plenum Publishing Corp.: New York, NY, USA, 1993; pp. 455–458.
101. Zheng, D.X.; Dong, L.; Huang, W.J.; Wu, X.H.; Nie, N. A review of imidazolium ionic liquids research and development towards working pair of absorption cycle. *Renew. Sust. Energ. Rev.* **2014**, *37*, 47–68. [[CrossRef](#)]
102. Green, M.D.; Long, T.E. Designing Imidazole-Based Ionic Liquids and Ionic Liquid Monomers for Emerging Technologies. *Polym. Rev.* **2009**, *49*, 291–314. [[CrossRef](#)]
103. Domanska, U.; Marciniak, A. Solubility of ionic liquid [emim][PF₆] in alcohols. *J. Phys. Chem. B* **2004**, *108*, 2376–2382. [[CrossRef](#)]
104. Heintz, A. Recent developments in thermodynamics and thermophysics of non-aqueous mixtures containing ionic liquids. A review. *J. Chem. Thermodyn.* **2005**, *37*, 525–535. [[CrossRef](#)]
105. Sahandzheeva, K.; Tuma, D.; Breyer, S.; Kamps, A.P.S.; Maurer, G. Liquid-liquid equilibrium in mixtures of the ionic liquid 1-n-butyl-3-methylimidazolium hexafluorophosphate and an alkanol. *J. Chem. Eng. Data* **2006**, *51*, 1516–1525. [[CrossRef](#)]
106. Pereiro, A.B.; Rodriguez, A. Study on the phase behaviour and thermodynamic properties of ionic liquids containing imidazolium cation with ethanol at several temperatures. *J. Chem. Thermodyn.* **2007**, *39*, 978–989. [[CrossRef](#)]
107. Abdulagatov, I.M.; Tekin, A.; Safarov, J.; Shahverdiyev, A.; Hassel, E. Densities and excess, apparent, and partial molar volumes of binary mixtures of BMIMBF₄ plus ethanol as a function of temperature, pressure, and concentration. *Int. J. Thermophys.* **2008**, *29*, 505–533. [[CrossRef](#)]
108. Domanska, U. Solubilities and thermophysical properties of ionic liquids. *Pure Appl. Chem.* **2005**, *77*, 543–557. [[CrossRef](#)]
109. Guo, Y.M.; Wang, X.; Tao, X.Y.; Shen, W.G. Liquid-liquid equilibrium and heat capacity measurements of the binary solution {ethanol+1-butyl-3-methylimidazolium hexafluorophosphate}. *J. Chem. Thermodyn.* **2017**, *115*, 342–351. [[CrossRef](#)]

110. Varela, L.M.; Mendez-Morales, T.; Carrete, J.; Gomez-Gonzalez, V.; Docampo-Alvarez, B.; Gallego, L.J.; Cabeza, O.; Russina, O. Solvation of molecular cosolvents and inorganic salts in ionic liquids: A review of molecular dynamics simulations. *J. Mol. Liq.* **2015**, *210*, 178–188. [[CrossRef](#)]
111. Secundo, F.; Carrea, G.; Tarabiono, C.; Gatti-Lafranconi, P.; Brocca, S.; Lotti, M.; Jaeger, K.E.; Puls, M.; Eggert, T. The lid is a structural and functional determinant of lipase activity and selectivity. *J. Mol. Catal. B Enzym.* **2006**, *39*, 166–170. [[CrossRef](#)]
112. Khan, F.I.; Lan, D.; Durrani, R.; Huan, W.; Zhao, Z.; Wang, Y. The lid domain in lipases: Structural and functional determinant of enzymatic properties. *Front. Bioeng. Biotechnol.* **2017**, *5*, 16. [[CrossRef](#)]
113. Kazlauskas, R.J.; Weissfloch, A.N.E.; Rappaport, A.T.; Cuccia, L.A. A rule to predict which enantiomer of a secondary alcohol reacts faster in reactions catalysed by cholesterol esterase, lipase from *Pseudomonas cepacia*, and lipase from *Candida rugosa*. *J. Org. Chem.* **1991**, *56*, 2656–2665. [[CrossRef](#)]
114. Borreguero, I.; Sánchez-Montero, J.M.; Sinisterra, J.V.; Rumbero, A.; Hermoso, J.A.; Alcántara, A.R. Regioselective resolution of 1,n-diols catalysed by lipases: A rational explanation of the enzymatic selectivity. *J. Mol. Catal. B Enzym.* **2001**, *11*, 1013–1024. [[CrossRef](#)]
115. Borreguero, I.; Sinisterra, J.V.; Rumbero, A.; Hermoso, J.A.; Martínez-Ripoll, M.; Alcántara, A.R. Acyclic phenylalkanedioles as substrates for the study of enzyme recognition. Regioselective acylation by porcine pancreatic lipase: A structural hypothesis for the enzymatic selectivity. *Tetrahedron* **1999**, *55*, 14961–14974. [[CrossRef](#)]
116. Filice, M.; Romero, O.; Abian, O.; de las Rivas, B.; Palomo, J.M. Low ionic liquid concentration in water: A green and simple approach to improve activity and selectivity of lipases. *RSC Adv.* **2014**, *4*, 49115–49122. [[CrossRef](#)]
117. Maraite, A.; Hoyos, P.; Carballeira, J.D.; Cabrera, Á.C.; Ansorge-Schumacher, M.B.; Alcántara, A.R. Lipase from *Pseudomonas stutzeri*: Purification, homology modelling and rational explanation of the substrate binding mode. *J. Mol. Catal. B Enzym.* **2013**, *87*, 88–98. [[CrossRef](#)]
118. Min, B.; Park, J.; Sim, Y.K.; Jung, S.; Kim, S.H.; Song, J.K.; Kim, B.T.; Park, S.Y.; Yun, J.; Park, S.; et al. Hydrogen-bonding-driven enantioselective resolution against the Kazlauskas rule to afford gamma-amino alcohols by *Candida rugosa* lipase. *ChemBioChem* **2015**, *16*, 77–82. [[CrossRef](#)]
119. Nascimento, P.A.M.; Pereira, J.F.B.; Santos-Ebinuma, V.D. Insights into the effect of imidazolium-based ionic liquids on chemical structure and hydrolytic activity of microbial lipase. *Bioprocess. Biosyst. Eng.* **2019**, *42*, 1235–1246. [[CrossRef](#)] [[PubMed](#)]
120. Palomo, J.M.; Fernandez-Lorente, G.; Guisan, J.M.; Fernandez-Lafuente, R. Modulation of immobilized lipase enantioselectivity via chemical amination. *Adv. Synth. Catal.* **2007**, *349*, 1119–1127. [[CrossRef](#)]



© 2020 by the authors. Licensee MDPI, Basel, Switzerland. This article is an open access article distributed under the terms and conditions of the Creative Commons Attribution (CC BY) license (<http://creativecommons.org/licenses/by/4.0/>).